STUDIES ON TWO-DIMENSIONAL TRANSONIC FLOWS OF COMPRESSIBLE FLUID.—PART I*

BY

S. TOMOTIKA AND K. TAMADA

University of Kyoto, Japan

1. Introduction. It is well-known that when the flow is everywhere subsonic in a field of flow, the nature of the two-dimensional isentropic flow of a compressible perfect fluid differs only slightly from that of the corresponding flow of an incompressible perfect fluid. Thus, in such a case, we can calculate the field of flow by any of the well-known methods of approximation. On the other hand, if the flow is supersonic throughout the field, we can determine the flow pattern by the method of characteristics.

Difficulty occurs, however, in the calculation of transonic flows which contain both subsonic and supersonic regions. The difficulty arises from the fact that the fundamental non-linear differential equation governing the field of flow changes from the elliptic type in the subsonic region to the hyperbolic type in the supersonic region.

Up to the present time, several writers have succeeded in finding exact solutions of the fundamental differential equation in certain particular cases, and they have thus obtained exact flow patterns of the compressible perfect fluid which afford valuable information on the complicated character of transonic flow. However, no exact solutions have yet been found which may be used to represent the accelerated-decelerated flow of gas through a nozzle.

In the present paper, an attempt is made to clarify some of the important features of transonic flow. To do this, we introduce a hypothetical gas which approximates the real gas, subject to the adiabatic law, in the vicinity of the critical state where the fluid velocity becomes just equal to the velocity of sound. Then, starting from the equations of motion (in two dimensions) of a compressible perfect fluid, we derive a partial differential equation for determining, in an exact manner, the flow of this hypothetical gas. This differential equation assumes a rather simple form, but retains the non-linearity of the original equations. Furthermore, it changes from the elliptic to the hyperbolic type when the fluid velocity becomes greater than the speed of sound.

We find that our fundamental non-linear equation can be solved exactly in several cases. Some of these solutions give us the flow through nozzles of various shapes. Here, we thoroughly discuss two flow patterns. By close examination of these flow patterns, we find some important and interesting features which are expected to be common to other similar transonic flows.

In a subsequent paper, an alternative method of treatment will be developed on the basis of the fundamental equations in the hodograph plane. Just as in the case of the adiabatic flow of the real gas, the fundamental differential equation for determining the flow of our hypothetical gas becomes linear in the hodograph plane. We have discovered a group of interesting particular solutions of this linear differential equation, which have points of singularity of various orders in the subsonic region of the hodograph plane. Thus, by suitable linear combinations of these particular solutions we can obtain various flow patterns with a uniform flow at infinity.

*Received Jan. 21, 1949. The investigations described in Parts I and II of the present paper were accomplished in 1946, while the main part of Part III was worked out before the end of March, 1947.

Although the hypothetical gas employed here has the advantage that the fundamental equations are simple and can be solved exactly, it can approximate the real gas only for a limited range of speeds. Thus, this method has the disadvantage that it is applicable only to nearly uniform transonic flows. In a subsequent paper, a theory is developed which can be applied to flows containing limited supersonic regions in the vicinity of an obstacle, as well as stagnation points. For this purpose, we introduce a second hypothetical gas and then discuss the subsonic uniform flow past an obstacle, making special reference to the so-called Taylor problem: Is there any theoretical possibility of a continuous potential flow past an obstacle such that it flows uniformly at a great distance from the body and at the same time contains limited supersonic regions in the neighborhood of the obstacle?

2. The fundamental equations. As is well-known, the two-dimensional steady irrotational flow of a compressible perfect fluid is given by the following simultaneous differential equations:

$$\varphi_x = u = q \cos \theta, \qquad \varphi_y = v = q \sin \theta,$$

$$\psi_x = -\rho q \sin \theta, \qquad \psi_y = \rho q \cos \theta,$$

where (x, y) are the Cartesian coordinates in the plane of fluid motion, (u, v) are the rectangular components of the velocity at any point in the field of flow, the angle θ denotes the direction of the velocity vector, and φ and ψ are the velocity potential and the stream function, respectively. The velocity magnitude q and the density ρ are normalized to equal unity for the critical velocity. Considering x and y as functions of φ and ψ, we then have

$$x_\varphi = \frac{1}{q} \cos \theta, \qquad x_\psi = -\frac{1}{\rho q} \sin \theta,$$

$$y_\varphi = \frac{1}{q} \sin \theta, \qquad y_\psi = \frac{1}{\rho q} \cos \theta.$$

On eliminating both x and y, the equations of motion in the (φ, ψ)-plane become

$$\begin{aligned} \theta_\varphi &= \frac{\rho}{q} q_\psi , \\ \theta_\psi &= \frac{q}{\rho}\left(\frac{1}{c^2} - \frac{1}{q^2}\right) q_\varphi . \end{aligned} \tag{2.1}$$

Here, we have replaced $d\rho/dq$, using Bernoulli's equation in differential form, namely,

$$\frac{d\rho}{dq} = -\frac{\rho q}{c^2}, \tag{2.2}$$

where c is the speed of sound normalized to unity for the critical state.

3. A theory of nearly-uniform transonic flow. In the following we shall develop a theory of nearly-uniform transonic flow by considering a hypothetical gas which approximates the adiabatic behavior of the real gas in the vicinity of the critical state (where the fluid velocity becomes just equal to the speed of sound).

Now, let us introduce a new variable w, defined by

$$w = \int_1^q \frac{\rho}{q}\, dq. \tag{3.1}$$

Then the fundamental equations (2.1) can be put in the form

$$\begin{aligned} \theta_\varphi &= w_\psi , \\ \theta_\psi &= -X w_\varphi , \end{aligned} \tag{3.2}$$

where

$$X = \frac{q^2}{\rho^2}\left(\frac{1}{q^2} - \frac{1}{c^2}\right).$$

If the usual isentropic law is assumed for the change of state of the gas, we have

$$\begin{aligned} \rho &= \left(\frac{\gamma+1}{2} - \frac{\gamma-1}{2}\, q^2\right)^{1/(\gamma-1)}, \\ c &= \left(\frac{\gamma+1}{2} - \frac{\gamma-1}{2}\, q^2\right)^{1/2}, \end{aligned} \tag{3.3}$$

where γ is the ratio of specific heats of the gas. By substituting Eqs. (3.3) into the expression for X and making use of Eq. (3.1), we can expand $X(w)$ in powers of w:

$$\begin{aligned} X(w) &= X(0) + \left[\left(\frac{dX}{dq}\right)\left(\frac{dq}{dw}\right)\right]_{q=1} w + O(w^2) \\ &= -(\gamma+1)w + O(w^2). \end{aligned} \tag{3.4}$$

In the case of nearly-uniform transonic flow, the value of w is small. Consequently the term $O(w^2)$ on the right-hand side of Eq. (3.4) may be neglected, and the fundamental equations (3.2) can be written as

$$\begin{aligned} \theta_\varphi &= w_\psi , \\ \theta_\psi &= k(w^2)_\varphi , \qquad k = \frac{\gamma+1}{2} . \end{aligned} \tag{3.5}$$

Elimination of θ from these equations yields immediately the partial differential equation for determining w, in the form

$$(kw)_{\psi\psi} = \{(kw)^2\}_{\varphi\varphi} . \tag{3.6}$$

Equations (3.5) and (3.6) can only approximately represent the nearly-uniform transonic flow of the real gas obeying the adiabatic law. But they may be taken as the exact fundamental equations of motion for the flow of a hypothetical gas which obeys an appropriate law of change of state. This method of approach to the problem is preferable, because it is possible to discuss the field of flow with mathematical rigor.

Before proceeding further, we shall now investigate what sort of gas corresponds to

the fundamental equations (3.5) or (3.6). Comparing Eqs. (3.5) with Eqs. (3.2), it is readily found that the relation which specifies the hypothetical gas is given by

$$X = -2kw, \qquad k = \frac{\gamma + 1}{2}.$$

Thus, taking Eqs. (3.1) and (2.2) into account, we obtain the characteristic equation for our hypothetical gas in the form

$$\left\{\frac{q^2}{\rho}\left(\frac{1}{\rho q}\right)'\right\}' = 2k\,\frac{\rho}{q}. \tag{3.7}$$

If this equation be solved subject to the conditions $(\rho)_{q=1} = 1$ and $(\rho')_{q=1} = -1$, we

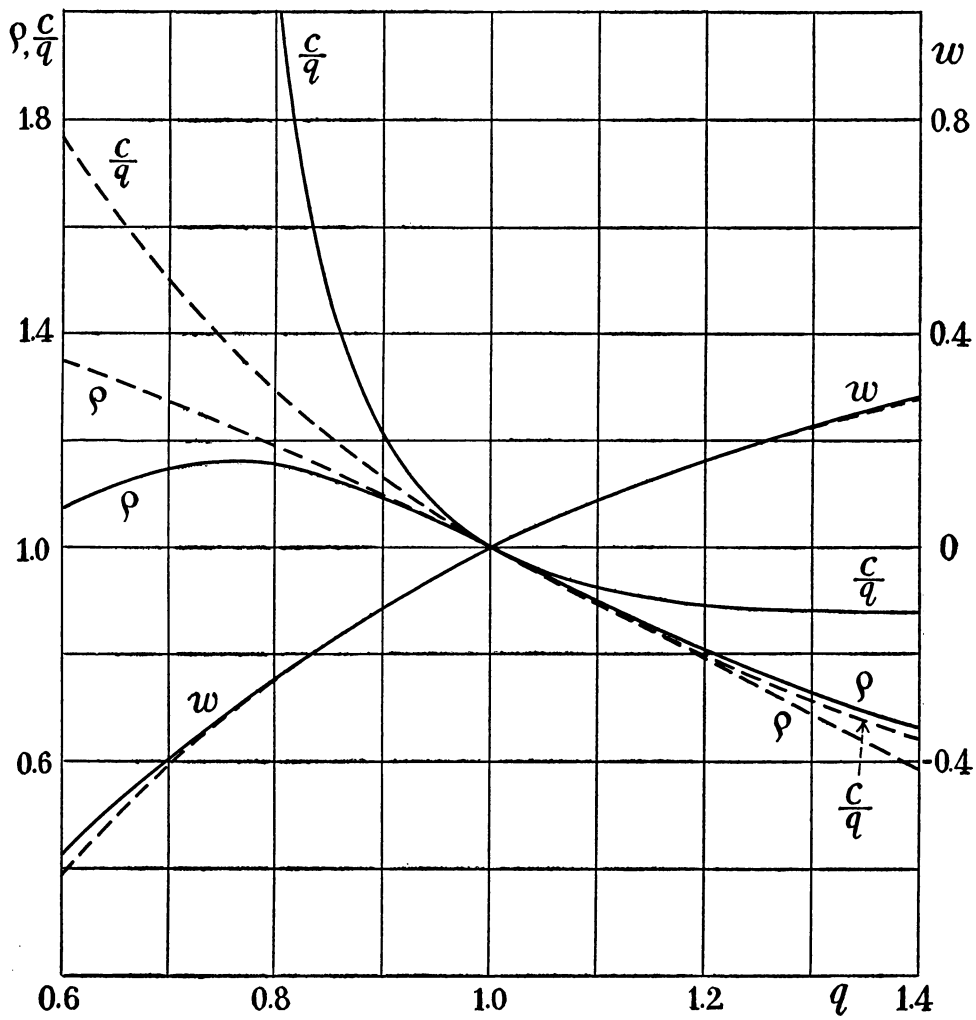

FIG. 1. Solid-line curves show the curves of w, c/q and ρ for the hypothetical gas used in the present paper, and dotted-line curves show the curves of the corresponding quantities for the real gas subject to the adiabatic law.

obtain the curve of $\rho(q)$ for our hypothetical gas, which coincides to the order of curvature at the critical state $q = 1$ with the corresponding curve of $\rho(q)$ for the real gas subject to the adiabatic law. The curves of $\rho(q)$, $c(q)$, and $w(q)$ for our hypothetical gas when $\gamma = 1.4$ are shown by solid-line curves in Fig. 1. The corresponding curves for the real gas obeying the adiabatic law are shown by dotted-line curves, for the sake of comparison.

4. Some exact solutions of the fundamental equation (3.6). The fundamental equation (3.6) for our hypothetical gas can be solved exactly by assuming kw in the following forms:

(a) $kw = f(\varphi + \lambda\psi)$, $\quad$ (λ = a certain constant)

(b) $kw = \Phi(\varphi) + \Psi(\psi)$,

(c) $kw = \Phi(\varphi)\Psi(\psi)$,

(d) $kw = \Psi_0(\psi) + \Psi_1(\psi)\varphi^2$,

(e) $kw = Z(\varphi + \psi^2) + 2\psi^2$,

where $Z(\varphi + \psi^2)$ denotes a function of $\varphi + \psi^2$.

These solutions together with the corresponding flow patterns have been investigated in detail by the junior writer in his doctoral thesis.[1] Only a brief sketch of the results obtained for the first three cases will be given here, however. The remaining two cases will be discussed in some detail in the following sections.

The first exact solution (a) gives the so-called spiral flow. Since an exact solution giving the similar flow pattern for the fundamental equations of motion of the real gas is well-known, we can compare the two solutions. It has been found that the flow of our hypothetical gas approximates sufficiently accurately the flow of the real gas.

The second solution (b) represents the flow through a Laval nozzle (i.e., a converging and diverging nozzle), which changes from the subsonic state to the supersonic one as it passes through the narrowest cross section. The results have been compared with those of the approximate calculation due to Meyer[2] for the corresponding adiabatic flow, and excellent agreement has been found.

The third solution (c) also gives the flow through a nozzle having a straight axis. Detailed calculations have been carried out for the flow which contains both the curves of singularity, $J = 0$ and $J = \infty$, where

$$J = \frac{\partial(x, y)}{\partial(q, \theta)} = \frac{\partial(x, y)}{\partial(\varphi, \psi)} \frac{\partial(\varphi, \psi)}{\partial(q, \theta)}.$$

5. The flow through a nozzle with two contractions. Let us consider the fourth solution (d), of the form

$$kw = \Psi_0(\psi) + \Psi_1(\psi)\varphi^2. \tag{5.1}$$

[1]K. Tamada, *Studies on the two-dimensional flow of gas, with special reference to the flow through various nozzles*, to be published.

[2]Th. Meyer, *Über zweidimensionale Bewegungsvorgänge in einem Gas, das mit Überschallgeschwindigkeit strömt*, Dissertation Goettingen, 1908.

Substituting this into the fundamental equation (3.6), we obtain two differential equations for determining the functions $\Psi_0(\psi)$ and $\Psi_1(\psi)$. After considerable manipulation*, the solution for Ψ_1 can be shown to be

$$\Psi_1 = \lambda\wp(t + \omega_2), \qquad t = (2\lambda)^{1/2}\psi,$$

where λ and ω_2 are constants of integration, and $\wp$ is the Weierstrass elliptic function.[3] The quantity ω_2 is chosen to equal the real half-period of the $\wp$-function so that the

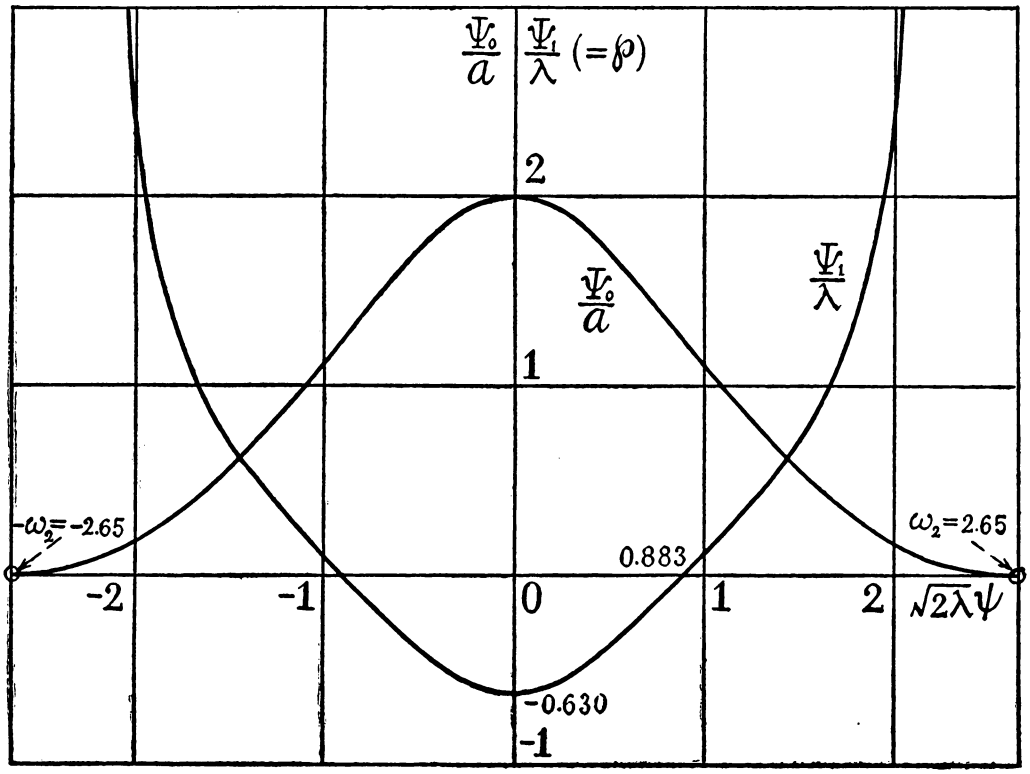

FIG. 2. Case when $g_3 = -1$.

flow may be symmetrical about the central streamline $\psi = 0$. With this result for Ψ_1, the function Ψ_0 becomes

$$\Psi_0 = a\left\{\left(1 + \frac{d\wp}{dt}\right)^{1/3} + \left(1 - \frac{d\wp}{dt}\right)^{1/3}\right\}$$

or

$$\Psi_0 = 2^{4/3}a\wp^{1/2}\cos\left(\frac{1}{3}\arctan\frac{d\wp}{dt}\right)$$

according as the invariant g_3 of the $\wp$-function is taken equal to -1 or $+1$.

*Since this flow will be of less technical interest than that of case (e), we omit the manipulative details.

[3]For the Weierstrass elliptic function $\wp$ used here, see E. Jahnke and F. Emde, *Funktiontafeln mit Formeln und Kurven*, Teubner, Leipzig and Berlin, 2nd ed., 1933, p. 166.

Substituting the expression for w as given by (5.1) into the fundamental equations (3.5) and carrying out a simple calculation, we obtain the result that

$$k\theta = \frac{d\Psi_0}{d\psi}\varphi + \frac{1}{3}\frac{d\Psi_1}{d\psi}\varphi^3, \tag{5.2}$$

where an additive constant of integration has been omitted since θ is everywhere zero along the streamline $\psi = 0$.

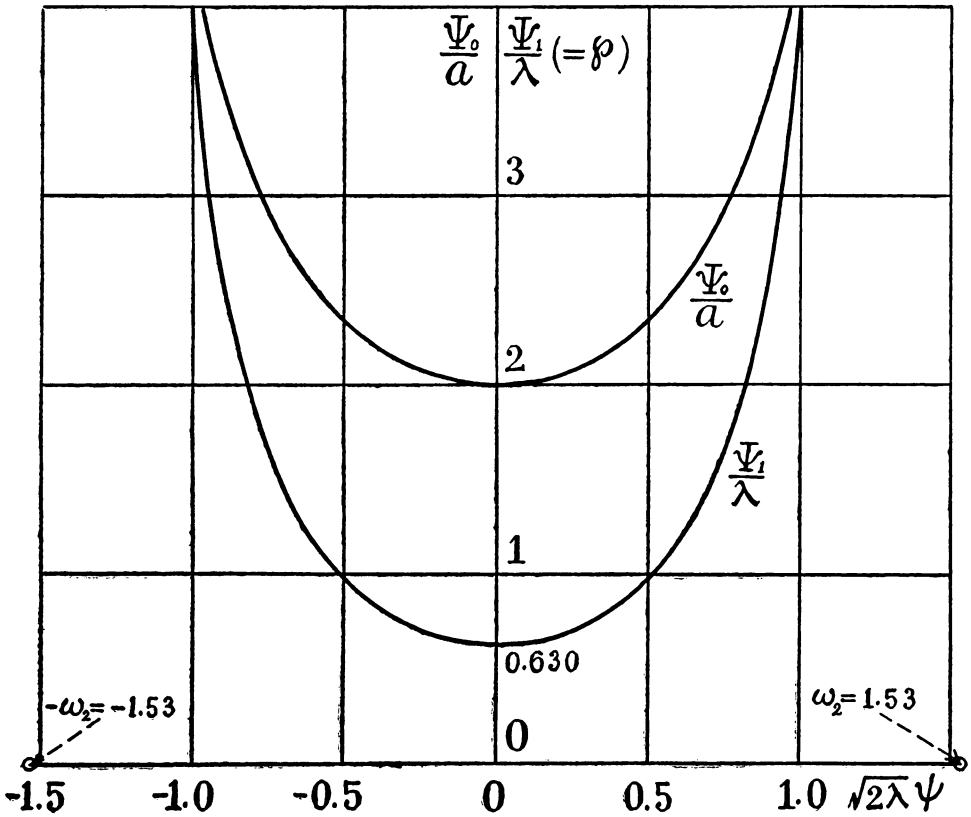

FIG. 3. Case when $g_3 = +1$.

The curves of Ψ_0 and Ψ_1 are shown in Fig. 2 for the case $g_3 = -1$ and in Fig. 3 for the case $g_3 = +1$. From these figures, in conjunction with Eqs. (5.1) and (5.2), it will be seen that the present solution gives different types of flow depending on the choice of signs for the constants g_3 and a.

Detailed numerical calculations have been carried out for the case $g_3 = -1$, by assuming $a = 0.15$, $\lambda = 0.5$ and taking, as usual, $\gamma = 1.4$ for air. Figure 4 shows the flow pattern in the physical plane and Fig. 5, the corresponding flow pattern in the hodograph plane. The correspondence between the physical and the hodograph planes can be easily understood, if we regard the streamlines in the hodograph plane as a group of contour lines forming twisted surfaces.

The flow pattern in the physical plane does not show any peculiarity, but, as is

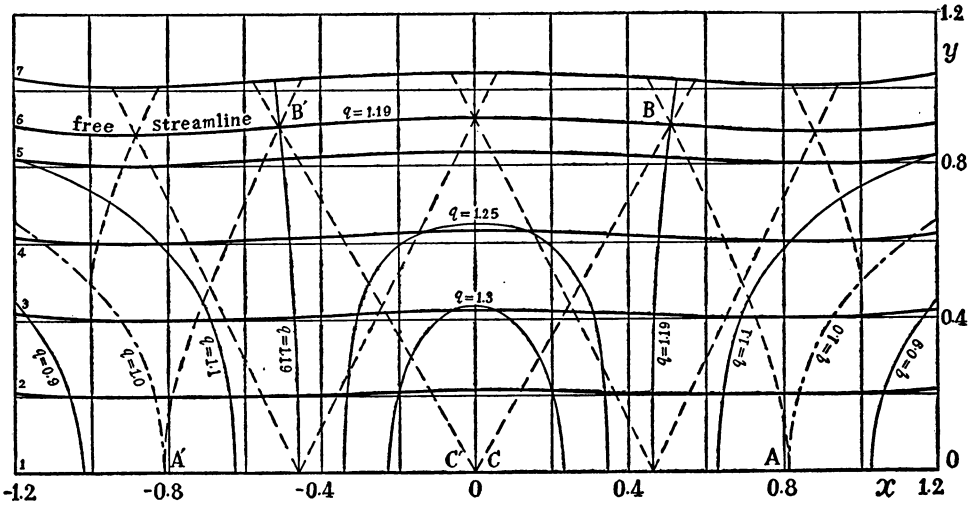

FIG. 4. Physical plane. Heavy solid-line curves and thin full-line curves represent streamlines and equi-velocity lines, respectively, while dotted-line curves represent Mach waves.

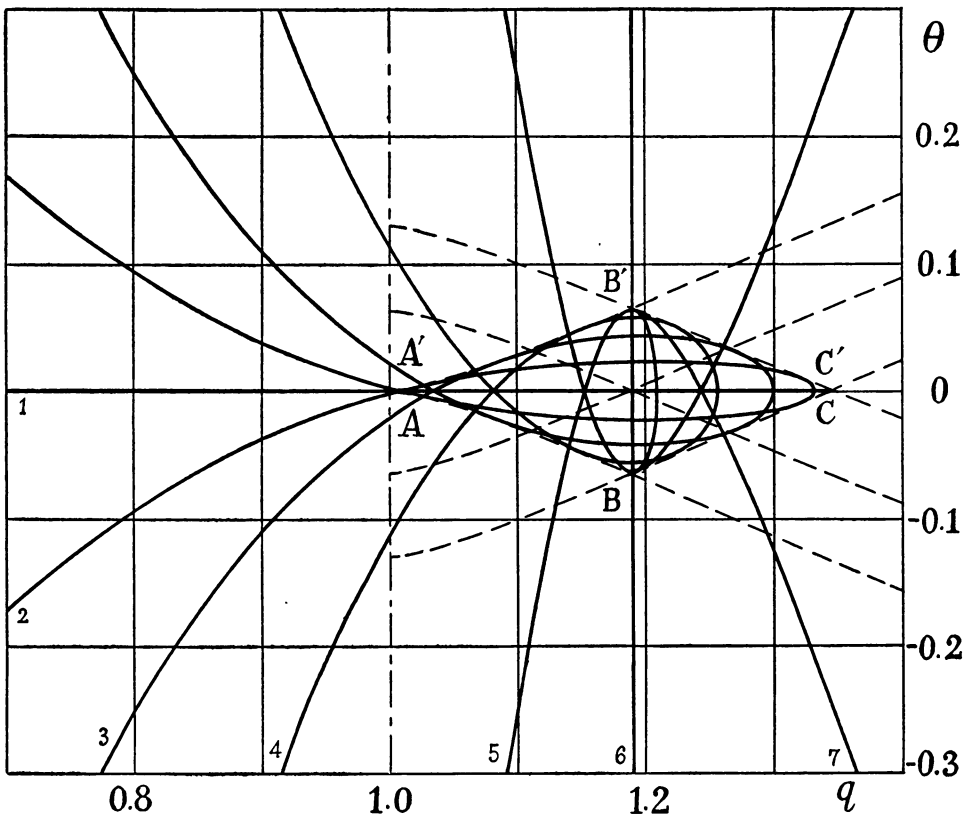

FIG. 5. Hodograph plane. Heavy solid-line curves represent streamlines, while dotted-line curves represent characteristics.

clearly seen from the flow pattern in the hodograph plane, it contains the particular Mach waves AB, $A'B'$,CB and $C'B'$ as the curves of singularity $J = \infty$.

6. Transition from the flow of Taylor's type to that of Meyer's in a given Laval nozzle. As the last example, we shall consider the flow represented by the fifth solution (e), of the form

$$kw = Z(u) + 2\psi^2, \tag{6.1}$$

where

$$u = \varphi + \psi^2.$$

Inserting this expression for w into the fundamental equation (3.6), we obtain the following equation for determining the function $Z(u)$:

$$\frac{d}{du}\left(Z\frac{dZ}{du}\right) - \frac{dZ}{du} - 2 = 0. \tag{6.2}$$

This equation can be integrated once immediately, and we get

$$Z\frac{dZ}{du} - Z - 2u = 0, \tag{6.3}$$

where a constant of integration has been included in u for the sake of convenience.

If we set $dZ/du = \chi$, it follows from Eq. (6.3) that

$$u = \frac{1}{2}(\chi - 1)Z. \tag{6.4}$$

Further, again taking into account that $dZ/du = \chi$ and $d^2Z/du^2 = \chi d\chi/dZ$, we have from Eq. (6.2) that

$$Z\chi\frac{d\chi}{dZ} = -(\chi - 2)(\chi + 1),$$

which can be integrated immediately to give

$$Z = 2^{2/3}a(\chi - 2)^{-2/3}(\chi + 1)^{-1/3}, \tag{6.5}$$

where $2^{2/3}a$ is a constant of integration. Eliminating χ from Eqs. (6.4) and (6.5), we get ultimately

$$(Z - 2u)^2(Z + u) = 2a^3. \tag{6.6}$$

Next, inserting the expression (6.1) for w into Eqs. (3.5) and carrying out simple integrations, we obtain the expression for θ in the form

$$k\theta = 2\psi\left(Z + 2\varphi + \frac{2}{3}\psi^2\right), \tag{6.7}$$

where a trivial constant of integration has been neglected.

From Eqs. (6.1), (6.6), and (6.7) it is seen that the flow under consideration is symmetrical about the straight streamline $\psi = 0$. Therefore, replacing two streamlines $\psi = \psi_0$ and $\psi = -\psi_0$ by two solid walls, we obtain a Laval nozzle having the line $\psi = 0$ as its axis.

Now, it is well-known that there may be two different types of flow in a given Laval

nozzle. In one type, the flow is subsonic on both sides of the throat of the nozzle but contains limited supersonic regions in the neighborhood of the walls at the throat (Fig. 6), while in the other the flow changes from a subsonic to a supersonic state as it passes through the throat (Fig. 7). The former type of flow was first discussed by Taylor

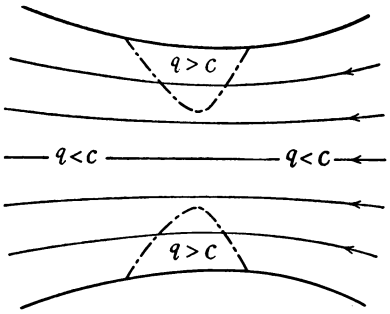

FIG. 6. Flow of Taylor's type.

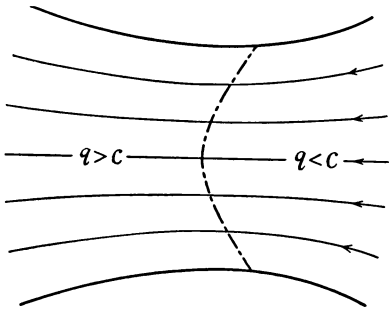

FIG. 7. Flow of Meyer's type.

and therefore will be called "Taylor's type". On the other hand, the latter type of flow was first investigated by Meyer in a paper already mentioned, and hence it may be conveniently referred to as "Meyer's type".

It is expected that under certain circumstances the transition from Taylor's to Meyer's type may occur in the flow through a Laval nozzle. The problem has already been investigated to some extent by Taylor[4], Görtler[5] and others. Unfortunately, however, these authors have not been able to arrive at any definite conclusion, since they have employed only approximate solutions in the form of series in x and y, which become rapidly divergent when the transition state is approached. It will be seen subsequently that it is possible by our present solutions to discuss the problem of transition from the flow of Taylor's type to that of Meyer's in a given Laval nozzle.

First, the values of the function $Z(u)$ must be calculated by using Eq. (6.6) in the cases $a > 0$ and $a < 0$. The curves of $Z(u)$ plotted against u are shown in Fig. 8. These curves represent the velocity distribution along the central axis $\psi = 0$ of the nozzle, since the function w, which is connected with q as shown in Fig. 1, becomes equal to Z when $\psi = 0$. It can be seen from these figures that the case $a < 0$ is suitable for our purpose of investigating the problem of transition of flow from Taylor's to Meyer's type in the Laval nozzle. In the case $a < 0$, the curve of Z consists of two branches A and B as indicated in Fig. 8. On the branch A, Z is always negative and becomes equal to $-\infty$ as $u \to \pm\infty$. Therefore, $kw = Z + 2\psi^2$ is everywhere negative (subsonic) for small values of $|\psi|$, but it becomes partly positive (supersonic) in some limited portions on those streamlines for which the values of $2\psi^2$ are larger than $|Z_{\max}| = |a|$. Thus, the solution in this case would give a flow pattern of Taylor's type as shown in Fig. 6.

As for the branch B, we first consider the range in which $Z < 0$. Then, it is seen from Fig. 8 that both Z and u increase as φ increases along any streamline $\psi =$ const.,

[4]G. I. Taylor, *The flow of air at high speeds past curved surfaces*, British A. R. C. Reports and Memoranda, No. 1381, 1931.

[5]H. Görtler, *Zum Übergang von Unterschall- zu Überschallgeschwindigkeit im Düsen*, Z. angew. Math. Mech. 19, 325-337 (1939).

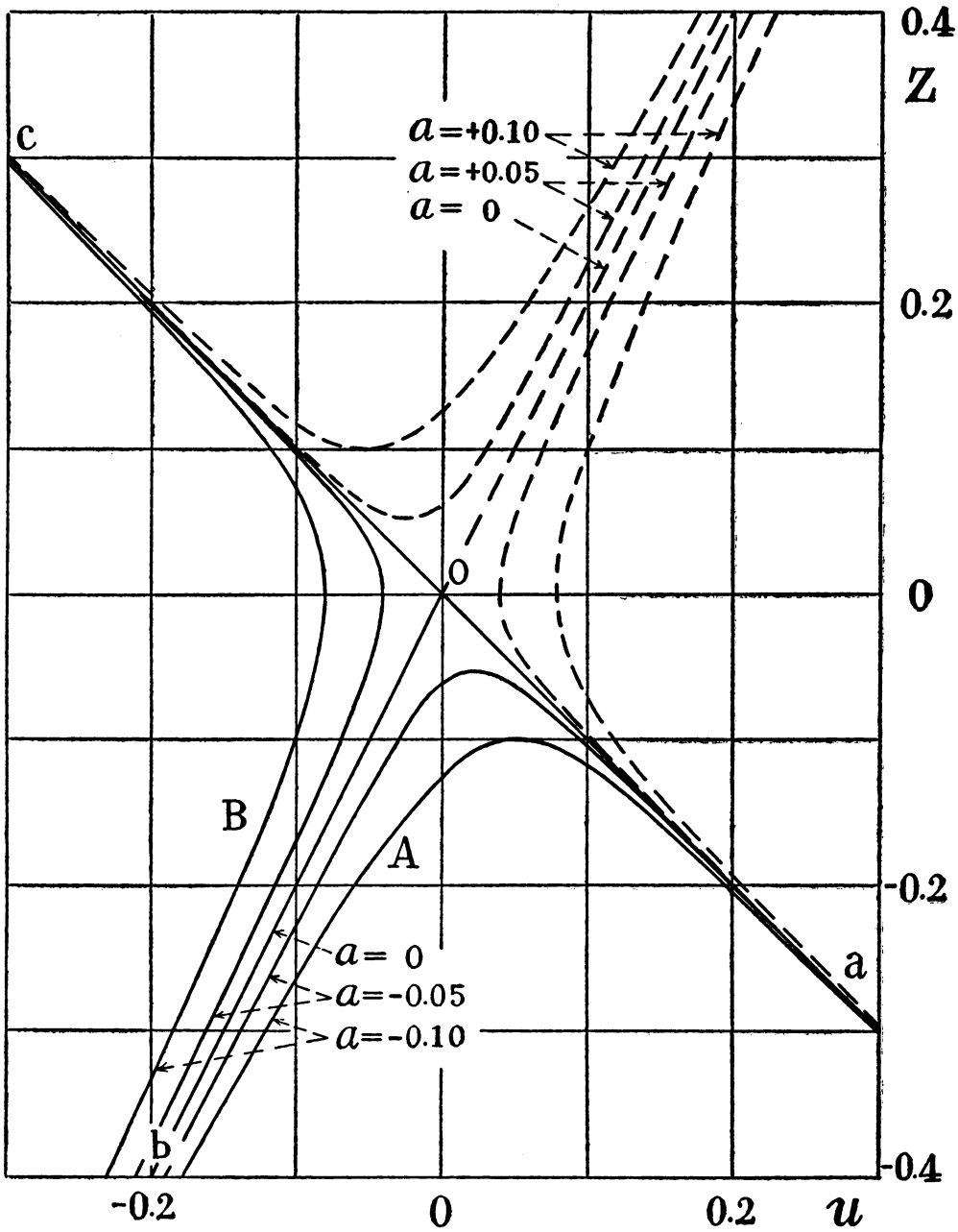

FIG. 8.

until the value of dZ/du becomes infinite at the point $u = u_0$, $Z = 0$. This means that the flow has reached the curve of singularity $J = 0$; for we have

$$J^{-1} = \frac{\partial(q, \theta)}{\partial(x, y)} = \frac{\partial(q, \theta)}{\partial(\varphi, \psi)} \frac{\partial(\varphi, \psi)}{\partial(x, y)}$$

$$= \rho^2 q \left\{ \frac{q^2}{\rho^2} \left(\frac{1}{c^2} - \frac{1}{q^2} \right) q_\varphi^2 - q_\psi^2 \right\} = \infty,$$

since q_φ and q_ψ are proportional to w_φ and w_ψ and hence contain dZ/du by Eqs. (3.1) and (6.1). Therefore, the flow in this case would be as shown in Fig. 9(a).

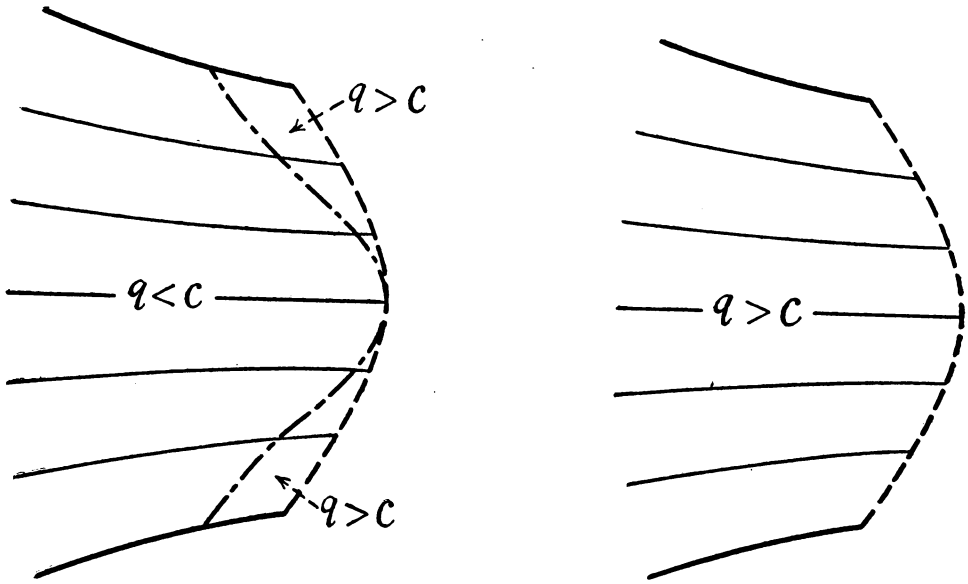

(a) (b)

FIG. 9.

For the range $Z > 0$ of the same branch B, we obtain a flow pattern as shown in Fig. 9(b), which is everywhere supersonic and has the curve of singularity $J = 0$ (the shock line) in common with the preceding flow in Fig. 9(a).

In the case $a = 0$, the branch A coincides with the two asymptotes $a0$ and $b0$. In this case, the local speed of sound is attained at some point (which corresponds to the point 0 in Fig. 8) on the axis of the nozzle; hence the upper and lower limited supersonic regions come in contact with each other at that point. This may be considered as the limiting case of the flow of Taylor's type. The flow pattern is as shown in Fig. 10(a).

In this case ($a = 0$), the branch B is also coincident with the asymptotes bO and cO ($=aO$) and hence the two branches A and B may be joined at O into one straight line aOc. If this branch aOc is adopted as Z, our solution would obviously give a flow pattern of Meyer's type as shown in Fig. 10(b), which has part of the flow pattern in common with the preceding case in Fig. 10(a), corresponding to the half-branch aO of Z. Figures 6 and 10 suggest a possible transition of flow from Taylor's to Meyer's type in the Laval nozzle.

Taylor and Görtler have treated the flow between two rigid circular walls symmetrical with respect to the x-axis. The dimensions of their nozzle were determined to satisfy the condition

$$R = 4h \tag{6.8}$$

at the throat of the nozzle, where R denotes the radius of curvature of the walls[6] and h is the half-breadth of the throat.

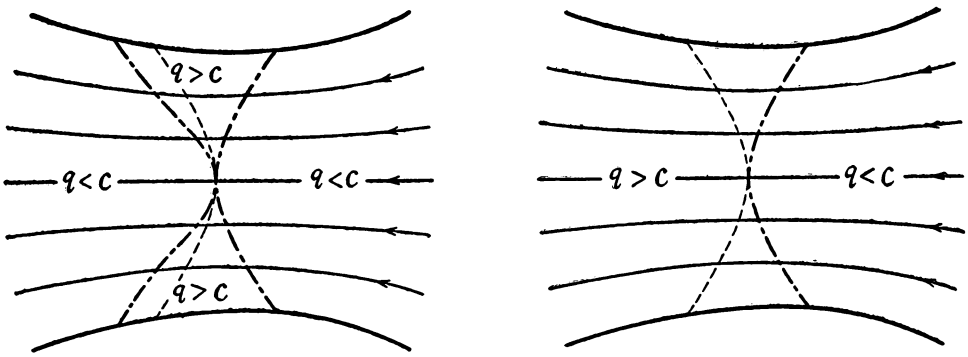

(a) (b)

FIG. 10.

For the sake of convenience, we shall use the same condition to specify the shape of the nozzle.[7] This condition determines the particular streamlines to be chosen as the walls of the nozzle, for given values of the parameter a. As will be seen presently, these streamlines are almost coincident over a considerably wide range of x, for the several values of a. Thus, our nozzle retains approximately a fixed shape in spite of the change of flow, and, therefore, we can discuss the problem of the transition from Taylor's to Meyer's type of flow in a given Laval nozzle.

Now, at the point (φ_0, ψ_0) on the wall at the throat of the nozzle, θ is obviously zero and hence we have, from Eq. (6.7), that

$$Z = -2\varphi_0 - \frac{2}{3}\psi_0^2 . \tag{6.9}$$

Remembering that $y_\psi = \cos\theta/\rho q$ the half-breadth of the throat of the nozzle is given by

$$h = \int_0^{\psi_0} \left(\frac{1}{\rho q}\cos\theta\right)_{\varphi=\varphi_0} d\psi. \tag{6.10}$$

Now, the radius of curvature R of any streamline is given by

$$R = \frac{ds}{d\theta} = \frac{ds}{d\varphi}\frac{d\varphi}{d\theta} = \frac{1}{q(d\theta/d\varphi)} .$$

[6]In Taylor's and Görtler's cases, R is the radius itself of each circular wall.

[7]It may be remarked here that unlike Taylor's and Görtler's cases, the walls of our nozzle do not assume the exact circular shape.

By Eqs. (6.7) and (6.3), we have

$$\frac{d\theta}{d\varphi} = \frac{2\psi}{k}\left(3 + \frac{2u}{Z}\right).$$

Therefore,

$$R = \frac{kZ}{2q\psi(3Z + 2u)}. \tag{6.11}$$

Thus, taking into account Eq. (6.9) the radius of curvature at the point (φ_0, ψ_0) on the wall is given by

$$R = \frac{k(3\varphi_0 + \psi_0^2)}{12q_0\varphi_0\psi_0}, \tag{6.12}$$

where q_0 is the value of q at the point (φ_0, ψ_0). In the present case, if use is made of Eq. (6.10), the condition (6.8) can be expressed in the form

$$\frac{k(3\varphi_0 + \psi_0^2)}{12q_0\varphi_0\psi_0} = 4\int_0^{\psi_0}\left(\frac{1}{\rho q}\cos\theta\right)_{\varphi=\varphi_0} d\psi. \tag{6.13}$$

If the two equations (6.9) and (6.13) are solved by the method of successive approximations, the values of φ_0 and ψ_0 for various values of a can be determined. We have

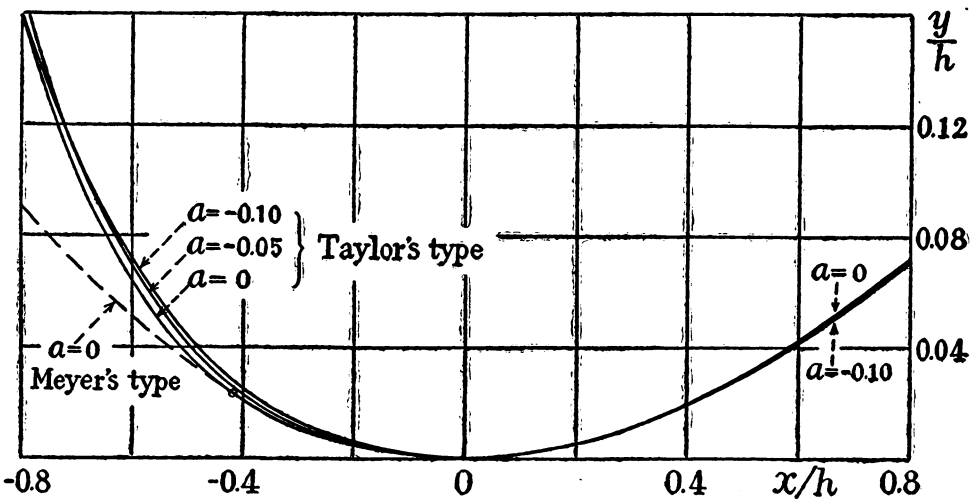

FIG. 11.

calculated the values of φ_0 and ψ_0 for three cases in which $a = -0.10$, $a = -0.05$ and $a = 0$, respectively, obtaining the results as shown in Table I.

Table I

a	-0.10	-0.05	0
φ_0	0.05028	0.04665	0.04605
ψ_0	0.3620	0.3707	0.3717

Figure 11 shows the shapes of the streamline $\psi = \psi_0$, which is to be replaced by the wall of the nozzle, as calculated for these three cases, by taking x/h and y/h as abscissa and ordinate, respectively, and choosing the point (φ_0, ψ_0) as the origin, the ordinate being shown on an enlarged scale. From this figure it will be seen that there is very satisfactory coincidence between these streamlines and, moreover, that if we make adjustment by shifting slightly the respective origins for the cases $a = -0.10$ and $a = -0.05$, almost perfect coincidence can be obtained within the range of x/h shown.

Now, as already mentioned, when $a = 0$ our solution gives two flow patterns, namely, the limiting case of the flow of Taylor's type and the flow of Meyer's type, which in the upstream subsonic region are exactly the same. The dotted-line curve in Fig. 11

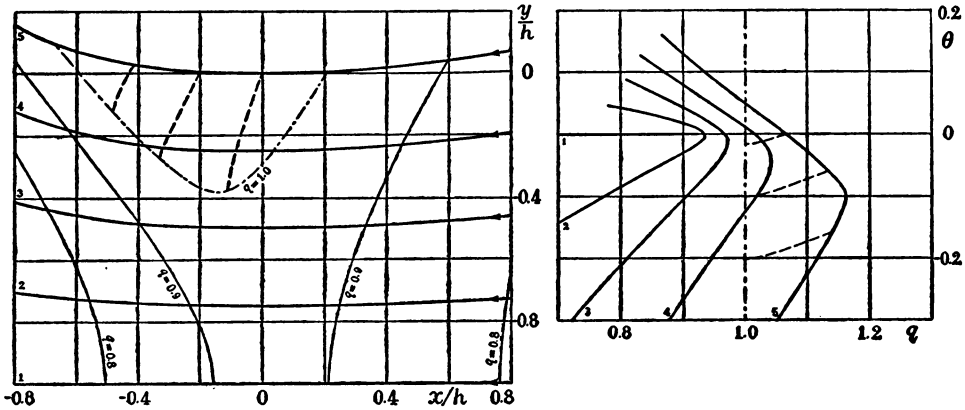

Physical plane. Hodograph plane.

FIG. 12. Heavy solid-line curves and thin solid-line curves represent streamlines and equi-velocity lines respectively, while dotted-line curves represent Mach waves (characteristics): $a = -0.10$.

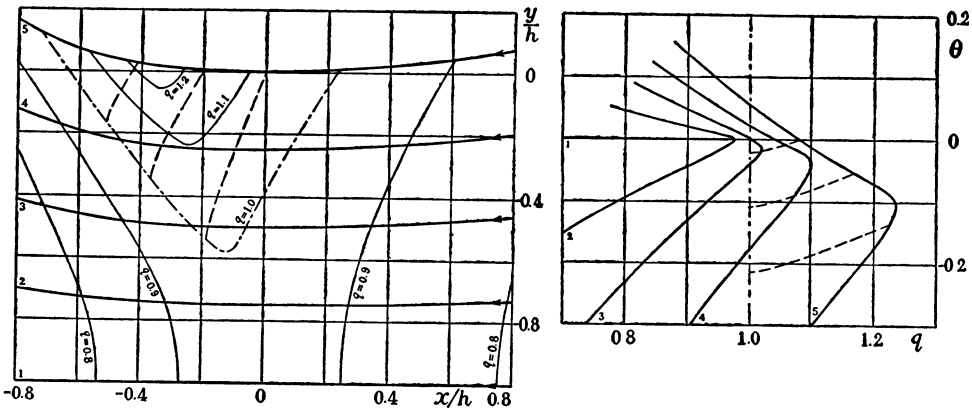

Physical plane. Hodograph plane.

FIG. 13. Heavy solid-line curves and thin solid-line curves represent streamlines and equi-velocity lines respectively, while dotted-line curves represent Mach waves (characteristics): $a = -0.05$.

shows the shape of the corresponding streamline for the case of the flow of Meyer's type. It is seen that the deviation of this curve from the group of curves corresponding to the case of the flow of Taylor's type becomes rather conspicuous in the supersonic

region on the left-hand side of the throat. However, this fact seems to have little effect on the discussion of the transition of flow, because in such a supersonic region, the wall can be continuously deformed by a small amount without causing any appreciable change in the upstream subsonic region.

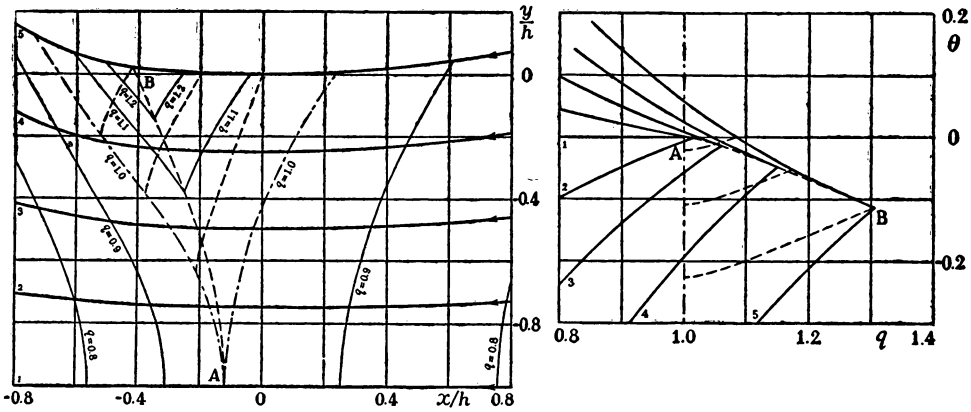

Physical plane. Hodograph plane.

FIG. 14. Heavy solid-line curves and thin solid-line curves represent streamlines and equi-velocity lines respectively, while dotted-line curves represent Mach waves (characteristics): $a = 0$.

We have calculated the flow patterns in the physical plane as well as in the hodograph plane, for the three above-mentioned cases, namely, $a = -0.10$, $a = -0.05$, and $a = 0$. The results are shown in Figs. 12-15. Also, the velocity distributions along the axis of the nozzle are shown in Fig. 16.

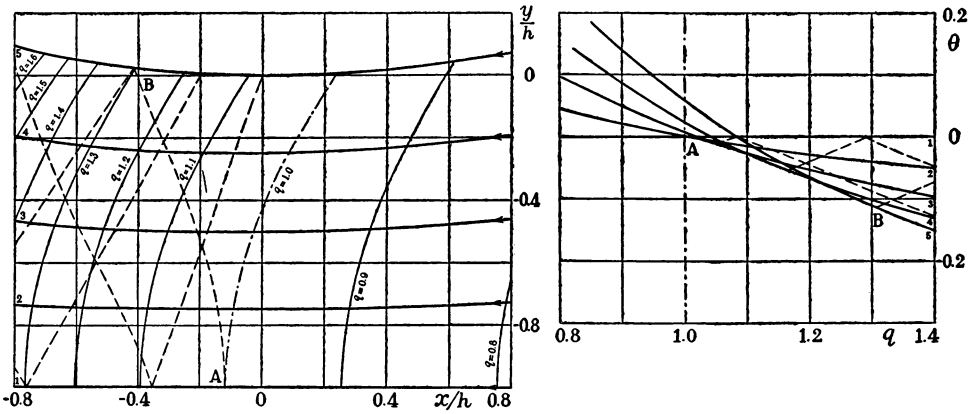

Physical plane. Hodograph plane.

FIG. 15. Heavy solid-line curves and thin solid-line curves represent streamlines and equi-velocity lines respectively, while dotted-line curves represent Mach waves (characteristics): $a = 0$.

Comparing these figures we can explain the possible transition of flow from Taylor's to Meyer's type in a given Laval nozzle in the following way. As the rate of flow increases, the curve of velocity distribution along a streamline becomes steeper until, in the limiting case of the flow of Taylor's type, it reaches an infinite curvature on a partic-

ular Mach wave AB (the curve of singularity $J = \infty$) as shown in Fig. 14. In this stage, the local speed of sound is first attained at some point A on the axis of the nozzle. At the same time the streamlines in the hodograph plane come in contact with a particular characteristic curve AB which corresponds to the Mach wave AB in the physical plane.

In the next stage, if the conditions governing the flow (such as the pressure at the outlet of the nozzle) be changed sufficiently, the flow changes abruptly to that of Meyer's type in the downstream region, having the Mach wave AB as the natural boundary of

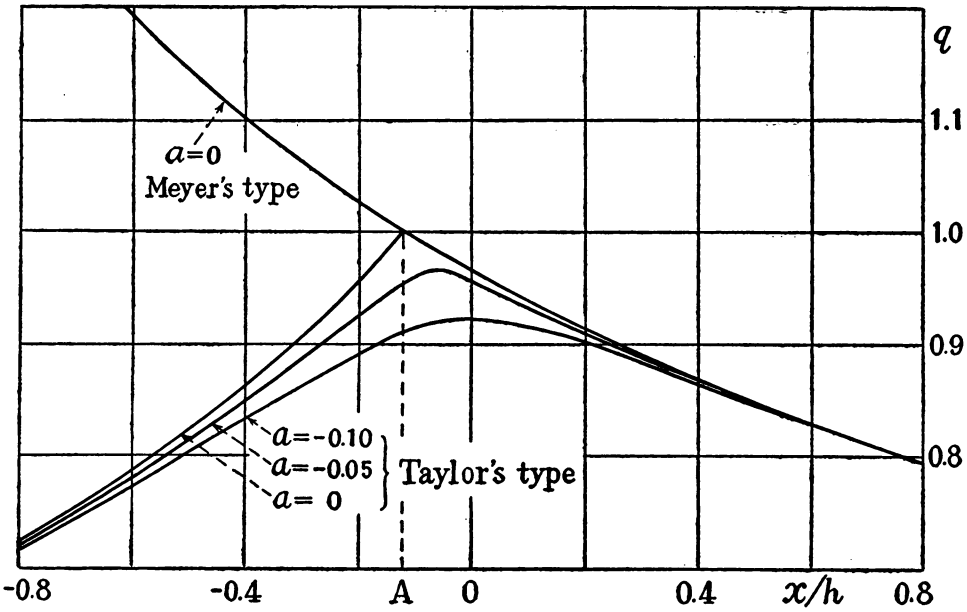

FIG. 16.

the unchanged upstream region. Such an abrupt change seems to be inherent in the flow, since the condition that the streamlines be in contact with some particular characteristic curve in the hodograph plane, in conjunction with the fixed shape of the wall of the nozzle, seems to determine the unique and isolated solution for the flow of Meyer's type. Moreover, the flow of Meyer's type cannot be approached in a continuous manner from the group of solutions for the flow of Taylor's type.

If the change of conditions controlling the flow is not sufficient for the occurrence of such an abrupt change of state, then intermediate stages occur in which the flow forms shock waves in the downstream side so as to fit the conditions at the outlet of the nozzle. At the beginning of these intermediate stages a slight shock wave first appears along the particular Mach wave AB (the curve of singularity $J = \infty$).